2008

Temperature dependency of burn-off emissions in the automobile industry

Krista Janette Scott
University of Iowa

TEMPERATURE DEPENDENCY OF BURN-OFF EMISSIONS IN THE AUTOMOBILE INDUSTRY

by

Krista Janette Scott

A thesis submitted in partial fulfillment
of the requirements of the Master of
Science degree in Occupational and Environmental Health (Industrial Hygiene)
in the Graduate College of
The University of Iowa

May 2008

Thesis Supervisor: Associate Professor William A. Heitbrink

Graduate College
The University of Iowa
Iowa City, Iowa

CERTIFICATE OF APPROVAL

_____

MASTER'S THESIS

_____

This is to certify that the Master's thesis of

Krista Janette Scott

has been approved by the Examining Committee
for the thesis requirement for the Master of Science
degree in Occupational and Environmental Health (Industrial Hygiene) at the
May 2008 graduation.

Thesis Committee: _____
William A. Heitbrink, Thesis Supervisor

_____
Thomas M. Peters

_____
Wayne T. Sanderson

ACKNOWLEDGEMENTS

I would like to thank God, first and foremost, for giving me the strength and determination to finish this thesis. I would also like to thank my mother for helping me to collect my data by being my personal scribe. I would like to thank Dr. Wayne Sanderson, Dr. William Heitbrink, and Dr. Thomas Peters for mentoring me through this process, without them this would not have been possible. I would like to thank Dan Simon for loaning me the Thermacam to collect my data and Gene White for providing metalworking fluids for my testing. I would also like to thank Ralph Altmaier, Tyler Sanderson, Craig Taylor, Michael Humann and Will Cyrs for lending a hand in the construction of my test chamber and Tyler Gunn for assisting in taking pictures during my project. I would like to thank Julia Venzke for helping me with my literature review; she really is a god send. And last but not least I would like to thank Ron Johnson for listening to me and offering good advice and assistance with the template during the process of thesis writing. This has truly been a unique and rewarding experience.

ABSTRACT

This work characterized burn-off emissions from automobiles. After an exhaustive literature review, engine temperatures were determined to reach a maximum temperature of approximately 110^{o}C, while exhaust system components reached a maximum temperature around 600^{o}C. Metal-drawing fluids were used to bend the exhaust system components during manufacturing. Because these components were not rinsed prior to incorporation into a vehicle, residues could be left on the surfaces. An experimental test chamber was constructed to conduct controlled testing of three metalworking fluids of various types to mimic real-world conditions. Real-time particle number measurements were made using a condensation particle counter and an optical particle counter. The temperature at which burn-off begins to occur was found to be around 120 to 150^{o}C. This burn-off was found to be an evaporation-condensation phenomenon when metalworking fluid residues vaporize and condense forming fine (0.1μm to 2.5μm) and ultrafine (<0.1μm) aerosols. The temperature dependency of this phenomenon was observed to follow the Clausius-Clapeyron equation that states as temperature increases, vapor pressure increases. Most aerosol particles were observed to be in the range of less than 0.01μm to approximately 2.0μm.

TABLE OF CONTENTS

LIST OF TABLES

LIST OF FIGURES

INTRODUCTION AND LITERATURE REVIEW

There are many recognized hazards in the automobile industry. These hazards include exposures to metals, chemicals, bioaerosols, physical agents such as noise and vibration, and ergonomic hazards such as awkward postures, forceful exertions, contact stresses and static postures. Exposure to airborne particles and vapors has been related to increased health risks such as: immune system suppression, respiratory inflammation, cardio-pulmonary disease, respiratory and chemical sensitivities, hypersensitivity pneumonitis, occupational asthma and bronchitis (O'Brien, 2003; NIOSH, 2007; McCawley et al., 2001; Kreyling et al., 2006; Detwiler-Okabaysahi and Schaper, 1996; Oberdörster, 2001; Park et al., 1996; Vincent and Clement, 2000; Anderson, 2000; Highwood and Kinnersley, 2006; Donldson, 2000; and Wichmann, 2000).

Burn-off emissions are a source of airborne particles and vapors generated in the process of automobile assembly. Vehicles are started in the final assembly and process area. Cars are driven on the chassis dynamometer at speeds approaching seventy miles an hour. During this process, a test system checks critical performance elements such as: brakes, power steering, and engine torque. Workers in this area have noticed "smoke" coming from the new cars and complained of eye and respiratory irritation. These emissions are believed to be fine and ultra-fine aerosols produced as the engine and associated exhaust components increase in temperature and residues left on their surfaces begin to vaporize. These aerosols may be created by evaporation and condensation, combustion, or a combination of the two.

Hot processes such as: welding, smelting, and refining of metals, vaporize material which then condenses to form small aerosol particles when rapidly cooled as it moves away from the high temperature zone (Vincent and Clement, 2000). As the temperature increases, more molecules have enough energy to escape the liquid phase and enter the gas phase or vaporize. As the temperature decreases away from the high

temperature zone, the forces of attraction between the molecules are strong enough to make the evaporated liquid return to the liquid phase. This is known as an evaporation-condensation phenomenon.

Combustion processes such as: transportation, carbon black manufacture, and coal-fired power plants also have the potential to produce ultrafine aerosols (Vincent and Clement, 2000). Combustion is a chemical reaction between a fuel and an oxidizer, generally oxygen, which generates heat and light. Incomplete combustion is involved where the fuel source is not entirely consumed. Both evaporation-condensation and combustion have a strong potential to produce large concentrations of fine and ultrafine particles.

Fine and Ultrafine Particles

The particles that are formed during the burn-off process are likely to be fine particles between 0.1μm to 2.5μm and ultrafine particles which are less than 0.1μm in size in all dimensions (Kreyling et al., 2006). According to the 2007 ACGIH TLV Booklet, particles in this size range (<2.5μm) are approximately 85-90% respriable particles. This means that most of these particles are able to enter the nose by normal breathing and can reach the alveolar regions deep in the lung, however only about 50% of the particles in the range from 0.01 to 0.03μm will deposit. Due to their size, many of these particles will follow the stream of air and be exhaled. Deposition of these particles in the pulmonary system will mostly be caused by diffusion; however, this deposition has a minimum between 0.1 and 1μm for the alveolar region (Ostiguy et al, 2006). Thoracic and extra-thoracic deposition increases as particle size decreases for particles smaller than approximately 0.006μm. After deposition in the lung, some ultrafine particles may elude alveolar macrophages and gain access to the pulmonary interstitium (Oberdörster, 2001). The number of particles and surface chemistry of fine and ultrafine particles play a role in their toxic properties. Due to the large surface area per given mass exposed on

ultrafine particles, greater contact occurs between ultrafine particles and respiratory tissue than occurs with larger particles. These small particles can also potentially carry other contaminants deep into the lung when inhaled or act as a catalyst for some intercellular reactions (Oberdörster, 2001). Although the mechanism is not entirely understood, ultrafines can be translocated to other organs such as the liver and heart (Wichmann and Peters, 2000; McCawley et al., 2001).

Ultrafine particles are different from nanoparticles because they are not created intentionally for a desired purpose. They are often produced from combustion and gas particle interactions in ambient and occupational environments. Therefore ultrafine particles are often complex in nature containing an abundance of compounds (Kreyling et al., 2006). In many workplace situations, ultrafine particle generation by evaporation-condensation is not feasible. When there are high vapor concentrations, the particles will generally grow out of the ultrafine range. Where there is a high number concentration, agglomeration can dominate to grow particles above 0.1μm (Vincent and Clement, 2000). This likelihood is also increased when there is generation of very small particles from the physical process of nucleation from the vapor phase. Nucleation can be heterogeneous where particles are formed by condensation onto existing nuclei or homogeneous nucleation and condensation from the gas back to the liquid phase (Vincent and Clement, 2000). Relatively low concentration of these particles must be present in order to prevent further coagulation. Localized heating enhances ultrafine aerosol formation because the temperature will decrease rapidly further from the source allowing the aerosol to essentially be "frozen" and no longer condense, nucleate or coagulate to form larger particles (Vincent and Clement, 2000).

There are various chemicals used in the manufacture of engine and exhaust system components that may leave a residue coating these surfaces. As vehicle surfaces increase in temperature after engine ignition, residual fluids have the potential to vaporize or combust, generating vapors and aerosols (see **Table 1-1)**. Vehicle engine blocks are

typically rinsed prior to being incorporated into a vehicle. This reduces the likelihood that chemical residues are left on the surface of the engine to vaporize when surface temperatures increase. However, the exhaust components are not rinsed prior to being incorporated into vehicles. Therefore, the metalworking fluids that are used to form these components may leave residue on the surface of the metal parts and be available for combustion or vaporization.

Metalworking Fluids

Metalworking fluids are the type of chemicals that are most likely to remain on newly manufactured vehicles. Metal working fluids is a name given to a group of fluids that are used to cool or lubricate metalwork during the machining process (NIOSH, 2006). Metalworking fluids are made in four main types from straight oils to synthetic fluids. The four main types of oils used in industry today in order from most commonly used to least are: soluble oils, semisynthetic fluids, synthetic fluids, and straight oils (STLE, 2006).

Soluble oils or emulsifiable oils are the most common type of metalworking fluid currently used in industry. These oils are made as a concentrate that is fortified with emulsifiers and specialty additives and are diluted with water forming an oil and water emulsion. The dilution percentage depends on the job task. For general machining and grinding dilutions to 1-20% of the concentrate are used. However, when used as a drawing compound and applied to metal before going into a press, less water is added such that dilutions to between 20-50% of the concentrate are used. At 50% dilution, the thickened dilution has superb lubricating properties and does not run off the metal prior to the draw (STLE, 2006). This class of metalworking fluids was created in response to a changeover to carbide tooling and increased machine speeds. A typical formulation of a soluble oil product is shown in **Table 1-2**.

Semisynthetic fluids are the next most common class of metalworking fluids used. This class is similar to soluble oils because they are also an emulsion. However, they are different because they are water-based like synthetic fluids. While the product concentrate is generally clear in appearance, it is generally 5 to 30% mineral oil emulsified into water. A typical formulation of a semisynthetic fluid is shown in **Table 1-3** (STLE, 2006).

Synthetic fluids are distinct because they contain no mineral oil. This allows them to provide excellent cooling properties due to the water content. However, because they contain so much water they also can cause corrosion. Therefore, a synthetic fluid will also contain a variety of rust inhibitors. A typical formulation of a synthetic fluid is shown in **Table 1-4** (STLE, 2006). While water based fluids have superior cooling properties than oil based fluids, they also allow for the growth of microbes (Detwiler-Okabayashi and Schaper, 1996). One study carried out by Schaper and Detwiler in 1991 showed that synthetic metalworking fluids produced both sensory and pulmonary irritation in mice. It could not be determined which component of the synthetic metalworking fluid was responsible for this irritation but the amines were the suspected cause (Detwiler-Okabayashi and Schaper, 1996).

Straight oils are petroleum or vegetable oils that are used without dilution with water. They can however, be compounded with various polar or chemically active additives (STLE, 2006). Lightweight solvents, neutral oils, and heavy bright and refined stocks are some of the most commonly used forms (STLE, 2006). Paraffinic oils have better oxidative stability and produce less smoke during cutting operations than naphthenic oils. Most compounded oils contain naphthenic oils because they are more compatible with lubricant additives (STLE, 2006). There is a potential for oils to be overheated and polynuclear hydrocarbons to be formed (NIOSH, 2006). These oils are generally used in the most difficult machining and forming operations. Their use has

greatly declined since its peak in the early 1940's (STLE, 2006). A typical straight oil formulation can be found in **Table 1-5**.

Evaporation-Condensation Phenomenon

Evaporation-condensation phenomenon is governed by the Clausius-Clapeyron equation, a fundamental law of nature that explains the equilibrium between two phases such as liquid and gas phases (Castellan, 1966; Poling et. al, 2000). When more vapor is present than allowed by the Clausius-Clapeyron equation then condensation will occur. If less vapor is present, evaporation will occur. As temperature increases, the saturation vapor pressure also increases. The Clausius-Clapeyron equation describes how this vapor pressure varies with temperature.

The relationship between saturation vapor pressure and temperature can be stated by the differential equation as follows:

$$\frac{d\ln(p)}{dT} = \frac{\Delta H}{RT^2} \qquad \text{(Eq. 1)}$$

where: p is the saturation vapor pressure, T is absolute temperature (^{o}K), ΔH is the latent heat of vaporization, and R is the gas law constant (1.987cal g-mol^{-1}^{o}K^{-1}). This equation is sometimes used to determine the latent heat of vaporization as a function of temperature.

To present vapor pressure data Equation 1 is integrated assuming heat of vaporization is relatively independent of temperature to yield the following formula:

$$\ln(p) = A - \frac{B}{T} \qquad \text{(Eq. 2)}$$

where: A is a constant, B is typically$\Delta H/R$, T is absolute temperature and the negative sign denotes that the enthalpy of vaporization is a negative number. This intergrated

form is sometimes used to present and summarize vapor pressure data as in the CRC Handbook (Lide, 1992).

Infrared Thermography

An infrared thermometer is actually a heat transfer sensor. It detects radiant heat transfer from the surface to the detector. The higher the temperature of an object the more infrared or thermal radiation emitted (Nicholas, J. V., 2001). Most thermal radiation is emitted perpendicular to the surface of an object so when measurement angles are less than 60^{o}, the amount of radiation decreases and erroneous low readings can occur (Nicholas, J. V., 2001).

This heat transfer is described as:

$$Q = \sigma A(eT_s{}^4 - aT_i{}^4) \quad \text{(Eq. 3)}$$

Where: Q = heat transfer (calories/second), σ= the Stefan-Boltzmann constant or $1.335x10^{-12}$cal sec^{-1} cm^{-2} $^{o}K^{-4}$, A=area (cm^2), e= emissivity of surface, T_s= temperature (^{o}K) at the surface, T_i= temperature at the instrument and a= absorptivity of the instrument (Bird, et al. 2004).

A high emissivity reading is necessary to get an accurate radiation to temperature correlation. Emissivity is strictly a surface phenomenon. It is essentially the ratio between the apparent temperature of the object, as measured by a radiation detector such as a thermal camera, and the actual temperature of an object. Under ideal conditions at equilibrium, the ability to emit or radiate energy is equal to the ability to absorb energy making emissivity another term for absorption (Nicholas, J. V., 2001). An industry standard used to estimate emissivity of an unknown surface is 3M electrical tape which has an emissivity of 0.94. Apparent temperature readings are taken on and off the surface of the tape until the two temperatures match (FLIR, 2007).

Study Objectives

The first objective of this study was to determine if burn-off emissions from metalworking fluid residue is an evaporation-condensation phenomenon as opposed to combustion or a combination of evaporation-condensation and combustion. The second objective was to determine at what temperature burn-off emissions become detectable over background concentrations. The third and final objective was to determine a general size distribution of the particles created by burn-off emissions.

Table 1-1 Automotive Temperature Extremes

Location	Typical Continuous Maximum Temperature
On engine transmission	140°C
At engine intake manifold	125°C
Under hood near engine	120°C
Under hood remote location	105°C
Exterior	70°C
Passenger compartment	70-80°C
In exhaust and combustion areas	200-600°C

Sources: Fairchild, Ray, M., Snyder, Rick B., Berlin, Carl W., Sarma, D. H. R.. "Emerging Substrate Technologies for Harsh-Environment Automotive Electronics Applications." Society of Automotive Engineers Technical Paper Series 2002-01-1052(2002):

Johnson, R. Wayne, Evans, John L. Jacobsen, Peter, Thompson, James R. (Rick), Christopher, Mark. "The Changing Automotive Environment: High-Temperature Electronics." IEEE Transactions on Electronics Packaging Manufacturing 27(2004): 164-176.

Table 1-2 Typical Formulation of a Soluble Oil Metalworking Fluid

Function	Component	% By Weight
Oil	100/100 naphthenic hydro-treated oil	68
Emulsifier	Sulfonate emulsifier base	17
EP lubricant	Chlorinated olefin	5
Boundary lubricant	Synthetic ester	5
Rust Inhibitor	Alkanolamide	3
Biocide	Phenol-type	2
	Total	100

Source: Society of Tribologists and Lubrication Engineers, Metalworking Fluids . 2. Wakefield: CRC Press Taylor & Francis, 2006.

Table 1-3 Typical Formulation of a Semisynthetic Metalworking Fluid

Function	Component	% By Weight
Emulsifier	Sulfonate base	5
Emulsifier	Alkanolamide	15
Oil	100/100 naphthenic oil	15
Corrosion inhibitor	Amine borate	6
Coupler	Butyl carbitol	1.5
Biocide/fungicide	Triazine/pyridinethione	2
Diluent	Water	55.5
	Total	100

Source: Society of Tribologists and Lubrication Engineers, Metalworking Fluids . 2. Wakefield: CRC Press Taylor & Francis, 2006.

Table 1-4 Typical Formulation of a Synthetic Metalworking Fluid

Function	Component	% By Weight
Diluent	Water	70
Rust inhibitor	Amine carboxylate	10
pH buffer and inhibitor	Triethanolamine	5
EP lubricant	Phosphate ester	4
Boundary lubricant	PEG ester	5
Boundary lubricant	Sulfated castor oil	4
Fungicide	Pyridinethione	2
	Total	100

Source: Society of Tribologists and Lubrication Engineers, Metalworking Fluids . 2. Wakefield: CRC Press Taylor & Francis, 2006.

Table 1-5 Typical Formulation of a Straight Oil Metalworking Fluid

Component	% By Weight
Naphthenic 100 s mineral oil	90
Lard oil	2
Chlorinated paraffin	6
Sulfurized lard oil	2
Total	100

Source: Society of Tribologists and Lubrication Engineers, Metalworking Fluids . 2. Wakefield: CRC Press Taylor & Francis, 2006.

TEMPERATURE DEPENDENCY OF BURN-OFF EMISSIONS IN THE AUTOMOBILE INDUSTRY

Introduction

The automobile industry has several recognized hazards. One of these hazards is burn-off emissions. Burn-off emissions are a source of airborne particles characterized as fine and ultra-fine aerosols produced as the engine and associated exhaust components increase in temperature and residues left on their surfaces begin to vaporize. Vehicles are started in the final assembly and process area and engine surfaces and exhaust system components reach operating temperatures for the first time. Workers in this area have noticed "smoke" coming from the new cars and complained of eye and respiratory irritation. These aerosols may be generated by evaporation and condensation, combustion, or a combination of the two.

Hot processes such as: welding, smelting, and refining of metals, vaporize material which then condenses to form small aerosol particles when rapidly cooled as it moves away from the high temperature zone (Vincent and Clement, 2000). As the temperature increases, more molecules have enough energy to escape the liquid phase and enter the gas phase or vaporize. As the temperature decreases away from the high temperature zone, the forces of attraction between the molecules are strong enough to make the evaporated liquid return to the liquid phase. This is known as an evaporation-condensation phenomenon.

Evaporation-condensation phenomenon is governed by the Clausius-Clapeyron equation, a fundamental law of nature that explains the equilibrium between two phases such as liquid and gas phases (Castellan, 1966; Poling et. al, 2000). When more vapor is present than allowed by the Clausius-Clapeyron equation then condensation will occur. If less vapor is present, evaporation will occur. As temperature increases, the saturation

vapor pressure also increases. The Clausius-Clapeyron equation describes how this vapor pressure varies with temperature.

The relationship between saturation vapor pressure and temperature can be stated by the differential equation as follows:

$$\frac{d \ln (p)}{dT} = \frac{\Delta H}{RT^2} \quad \text{(Eq. 1)}$$

where: p is the saturation vapor pressure, T is absolute temperature (^{o}K), ΔH is the latent heat of vaporization, and R is the gas law constant (1.987cal g-mol^{-1}^{o}K^{-1}). This equation is sometimes used to determine the latent heat of vaporization as a function of temperature.

To present vapor pressure data Equation 1 is integrated assuming heat of vaporization is relatively independent of temperature to yield the following formula:

$$\ln(p) = A - \frac{B}{T} \quad \text{(Eq. 2)}$$

where: A is a constant, B is typically$\Delta H/R$, T is absolute temperature and the negative sign denotes that the enthalpy of vaporization is a negative number. This integrated form is sometimes used to present and summarize vapor pressure data as in the CRC Handbook (Lide, 1992).

Combustion processes such as: transportation, carbon black manufacture, and coal-fired power plants also have the potential to produce ultrafine aerosols (Vincent and Clement, 2000). Combustion is a chemical reaction between a fuel and an oxidizer, generally oxygen, which generates heat and light. Incomplete combustion occurs where the fuel source is not entirely consumed. Both evaporation-condensation and combustion phenomena have a strong potential to produce large concentrations of fine and ultrafine particles.

The particles that are formed during the burn-off process are likely to be fine particles between 0.1µm to 2.5µm and ultrafine particles which are less than 0.1µm in size in all dimensions (Kreyling et al., 2006). The number of particles and surface chemistry of fine and ultrafine particles play a role in their toxic properties. Due to the large surface area per given mass exposed on ultrafine particles, greater contact occurs between ultrafine particles and respiratory tissue than occurs with larger particles. These small particles can also potentially carry other contaminants deep into the lung when inhaled or act as a catalyst for some intercellular reactions (Oberdörster, 2001).

There are various chemicals used in the manufacture of engine and exhaust system components that may leave a residue coating these surfaces. Metalworking fluids are the type of chemicals that are most likely to remain on newly manufactured vehicles. Metalworking fluids are made in four main types from straight oils to synthetic fluids. As vehicle surfaces increase in temperature after engine ignition, residual fluids have the potential to vaporize or combust, generating vapors and aerosols (see **Table 1-1)**. Engine temperatures generally do not exceed 110^{o}C, and exhaust system components can reach upwards of 600^{o}C (Fairchild et al., 2002, Johnson et al., 2004**)**.

To determine temperatures of various vehicle parts, infrared thermography is used. An infrared thermometer is actually a heat transfer sensor. It detects radiant heat transfer from the surface to the detector. The higher the temperature of an object the more infrared or thermal radiation emitted (Nicholas, J. V., 2001).

The first objective of this study was to determine if burn-off emissions from metalworking fluid residue is an evaporation-condensation phenomenon as opposed to combustion or a combination of evaporation-condensation and combustion. The second objective was to determine at what temperature burn-off emissions become detectable over background concentrations. The third and final objective was to determine a general size distribution of the particles created by burn-off emissions.

Methods and Materials

Objective and Overview

The goal of this experimental work was to determine the extent to which temperature explains the generation of aerosols from metalworking fluid residue on automotive exhaust system components. To conduct this experiment, a hotplate was placed inside a ventilated enclosure. A pan coated with 5 grams of metalworking fluid was set on the hotplate at various temperatures. Emissions and apparent temperatures were simultaneously measured. Apparent temperatures were measured with infrared thermography. Emissions were measured inside the ductwork downstream from the chamber with condensation particle counter (CPC) and an optical particle counter OPC). The data was analyzed to determine the temperature dependency of the burn-off emissions and to what extent these emissions are explained by the Clausius-Clapeyron equation.

Materials

Test chamber: A test chamber was constructed as pictorially shown in **Figure 2-1** and schematically in **Figure 2-2**. The test chamber was a square cube with dimensions of 4 feet on each side. The front of the chamber was a filter holder fitted with two 20”x30”x1” 3M Filtrete™ Ultra allergen reduction filters (Model 6132) and two 16”x20”x1” 3M Filtrete™ Ultra allergen reduction filters (Model 2000). The bottom was the concrete floor and the remaining four sides were Plexiglas with one door. A hole was cut in the back of the chamber to insert the ductwork, and a hole was cut in the top of the chamber to allow apparent temperature measurements. The hotplate (Model SP47235-60, Barnstead/Thermolyne, Dubuque, IA) was placed directly in front of the exhaust take-off as shown in **Figure 2-1** and **Figure 2-2**. An 18 inch square, 10 inch tall baffle was placed around the hotplate which is not shown in **Figure 2-1** and **Figure 2-2**.

The ductwork had two 90^{o} elbows to ensure mixing and sampling was conducted 20 feet downstream of the inlet to the duct. The ductwork was connected to a large tube axial fan (TC-Axial, Type TCTA 4000CFM, Twin City Fan and Blower, Minneapolis, MN) which moved 2300 cubic feet per minute (CFM) through the chamber.

Spring pans: The test substances were placed on spring-form pans for testing (Springform pan, 4555, Fox Run Craftsmen, Ivyland, PA). These pans were painted spray-painted black (Special purpose high-heat and radiator paint, high heat black 1614, Krylon products group, Cleveland, OH) to use infrared thermography to track apparent temperatures.

Test fluids: Three metalworking fluids from Milacron were tested including both semi-synthetic oils and synthetic fluids as described in **Table 2-1** and **Table 2-2**.

Concentration and Temperature Measurement Devices

Condensation particle counter: A condensation particle counter (CPC, Model 3007, TSI Inc., Shoreview, MN) was used to count number concentrations of particles over a range of 0.01μm to greater than 1μm. Measurements were taken every second. To minimize coincidence errors, a diluter was fabricated by drilling a hole in the end cap of a cartridge filter (Hepacap 90406A, 6702-7500 E495, Whatman, Spingfield Mill, UK) (Peters, 2006). This reduced the concentration by a factor of 7.02.

Optical particle counter: An optical particle counter (OPC, PDM-1108, Grimm, Ainring, Germany), was used to measure airborne particle number concentration. The OPC sizes particles into 15 channels from 0.3 μm to 20 μm based upon the amount of light scattered. This device measured concentrations every 6 seconds. An isokinetic sampling probe (1.152 isokinetic sampling pipe, stainless steel, Grimm, Ainring, Germany) with an inlet diameter of 0.15cm was connected to the OPC.

Airflow: The average velocity in the chamber was measured using an inclined manometer (Durablock Manometer 400, Dwyer Instruments Inc., Michigan City, IN)

attached to a delta tube (Delta Tube 306AZ-11-A0, Midwest Instruments, Sterling Heights, MI). Air flow was set at 2300 cubic feet per minute (+/-200 CFM), by adjusting the blast gate.

Thermal infrared camera: A thermal infrared camera (Thermacam, PM390, FLIR Systems Inc., North Billerica, MA) was used to capture apparent temperatures. This camera measures infrared energy in the spectral band range from 3.4μm to 5μm and a temperature range from -10 to 450°C (-14 to 842°F) within +/- 2% or 2°C (FLIR, 1999). The emissivity on the camera was set to 0.95 for a painted black surface by following standard procedures used in the industry (FLIR, 2007). The thermal camera took measurements every 30 seconds during the experimental testing period.

Experimental Procedure

After painting, springform pans were allowed to dry. Each pan was weighed and the scale was zeroed with the pan on the scale. Each test substance was added to the pan using a weigh boat and a spatula until 5.00g (+/-0.02g) was evenly distributed. Five temperature settings were selected (2, 4, 6, 8, and 10) and three replicates were made at each temperature setting. The fan was turned on and the hotplate temperature was adjusted to the appropriate setting and allowed to preheat. During this process the CPC and OPC began logging data on two laptop computers. Ambient temperature and relative humidity were collected using a Q-Trak (Q-Trak 8551, TSI Incorporated, St. Paul, MN). The thermal camera was attached to a television, the emissivity was set to 0.95, the relative humidity and ambient temperature were selected and images began to be captured. A pre-weight was recorded for each pan and test substance. After all the equipment was logging data, the pan was placed onto the hot hotplate and the chamber door was closed. Once data logging on the CPC began to reach equilibrium or reach a peak and then decline, the test substance was removed from the chamber and data acquisition was terminated. After cooling a post weight was taken. Change in color,

visible smoke production, and odor were all documented during each run. Picture number, pre and post-weights, substance weight added to plate, static pressure, temperature setting, relative humidity, ambient temperature, and file names were also documented for each test run. This procedure was followed for all substances.

Statistical Data Analysis

Before analysis, the data was censored to account for background aerosol concentration. This was done by averaging concentrations over a range where the concentration appeared to be independent of temperature. Verification was provided by performing regression analysis with concentration as a function of temperature. The range where the slope of the regression line did not differ significantly from zero (p-value >0.05) was assumed to be background concentration. The mean (X) and standard deviation (s) of this range was computed. An upper tolerance limit (UTL) was computed for the background concentration as:

$$UTL = X + Ks \quad \text{(Eq. 4)}$$

where: K was obtained from the National Bureau of Standards Handbook such that at a 99% level of confidence, 99% of the background concentration is less than this value (Natrella, 1963).

For higher temperatures, the fluid was exhausted from the pan allowing aerosol formation from combustion. This data was excluded by examining data from individual runs plotted to fit the Clausius-Clapeyron equation. Where the slope of the Clausius-Clapeyron plot was positive, the data was excluded from the analysis.

The temperature and concentration measurements from all runs for each substance were assembled into a single data set. Then, the natural log (ln) of concentration was plotted as a function of temperature and the natural log of concentration was plotted as a function of reciprocal absolute temperature.

Regression analysis for these plots was performed using Excel data analysis pack for Microsoft Excel 2007. The concentration and temperature data was fit to two models:

$$ln(C) = a + bT_C \quad \text{(Eq. 5)}$$

$$ln(C) = a + \frac{b}{T_K} \quad \text{(Eq. 6)}$$

The regression tool from excel was also used to compute the following statistics: number of observations, the regression coefficients a and b, standard error for the regression line, the standard error for the regression coefficients and the fraction of the variability in natural log of concentration explained by the regression model (R^2). Standard errors explain the variability about the regression line and the regression coefficients (Dougherty, 1990).

Results

The intermediate data analysis results are presented in the Appendix. These include tables that present: regression statistics, temperature and concentration ranges for each run and test substance, health effects and regulations and chemical and physical properties of the three substances. There are also graphs of the 15 size channels from the OPC presented for each substance.

Plots of concentration as a function of temperature for each substance are shown in **Figures 2-3, 2-4** and **2-5**. **Table 2-1** shows the regression statistics from fitting the data to equation 5. Apparently, temperature explains much of the variability in the data as the R^2 values are greater than 0.80. Temperature ranges at which aerosol concentration exceeds background concentration (represented by the UTL) is presented in **Table 2-2**.

Clausius-Clapeyron plots or natural log of concentration as a function of reciprocal absolute temperature are shown in **Figures 2-6, 2-7** and **2-8**. The associated R^2 values are greater than 0.50. This indicates that vapor pressure explains

approximately 50% or more of the variability in the data. Regression statistics for this model are also presented in **Table 2-1**. Equation 2-1 seems to fit the data well. Equation 2-2 is the integrated form of the Clausius-Clapeyron equation.

Discussion

Background concentration in the assembly plant is likely to be much higher (at least 2 to 3 times) than those in the experiment, therefore the temperature needed to produce aerosol concentrations over background concentration is also higher. If background concentration is around 20,000 to 30,000 for an actual plant, then the temperatures required would be greater than 150^{o}C. As shown in T**able 1-1**, only exhaust system components reach temperatures in excess of 150^{o}C. The data presented in **Figure 2-6, Figure 2-7** and **Figure 2-8** suggest that vapor pressure explains much of the variability in the data. **Figures 2-3, 2-4 and 2-5** indicate a very strong temperature dependency.

Limitations of this study

Particle sizes less than 0.3µm could not be obtained for this data, so an accurate size distribution for ultrafine particles was not possible. Some temperatures were not represented in this experiment, limiting the scope of analysis. Higher temperatures were excluded because of substance exhaustion. Therefore higher temperatures were not analyzed.

Table 2-1 Regression Statistics for Hotspot Temperature Data

Figure Number	Substance Number	Number of Observations	Temperature Range	Slope	Slope Standard Error	R^2 Value	Adjusted R^2	Regression Line Standard Error	Intercept Coefficient	Intercept Standard Error
2-3	1	432	64-398	0.012	0.0002	0.85	0.85	0.45	8.00	0.05
2-4	2	382	69-410	0.018	0.0002	0.94	0.94	0.39	6.54	0.05
2-5	3	448	69-399	0.018	0.0003	0.91	0.91	0.47	6.82	0.06
2-6	1	130	220-377	-6898.04	274.59	0.83	0.83	0.43	21.68	0.50
2-7	2	109	220-410	-4287.38	248.45	0.74	0.51	0.45	17.68	0.44
2-8	3	168	220-342	-6660.12	337.59	0.70	0.70	0.46	22.41	0.64

Table 2-2 Temperatures Required to Exceed Background Concentration

Test Substance	Temperature Range	Upper Tolerance Limit for Background Aerosol
Substance 1	120-150^{o}C	14665 #/cm^{3}
Substance 2	100-140^{o}C	4386 #/cm^{3}
Substance 3	100-130^{o}C	6556 #/cm^{3}

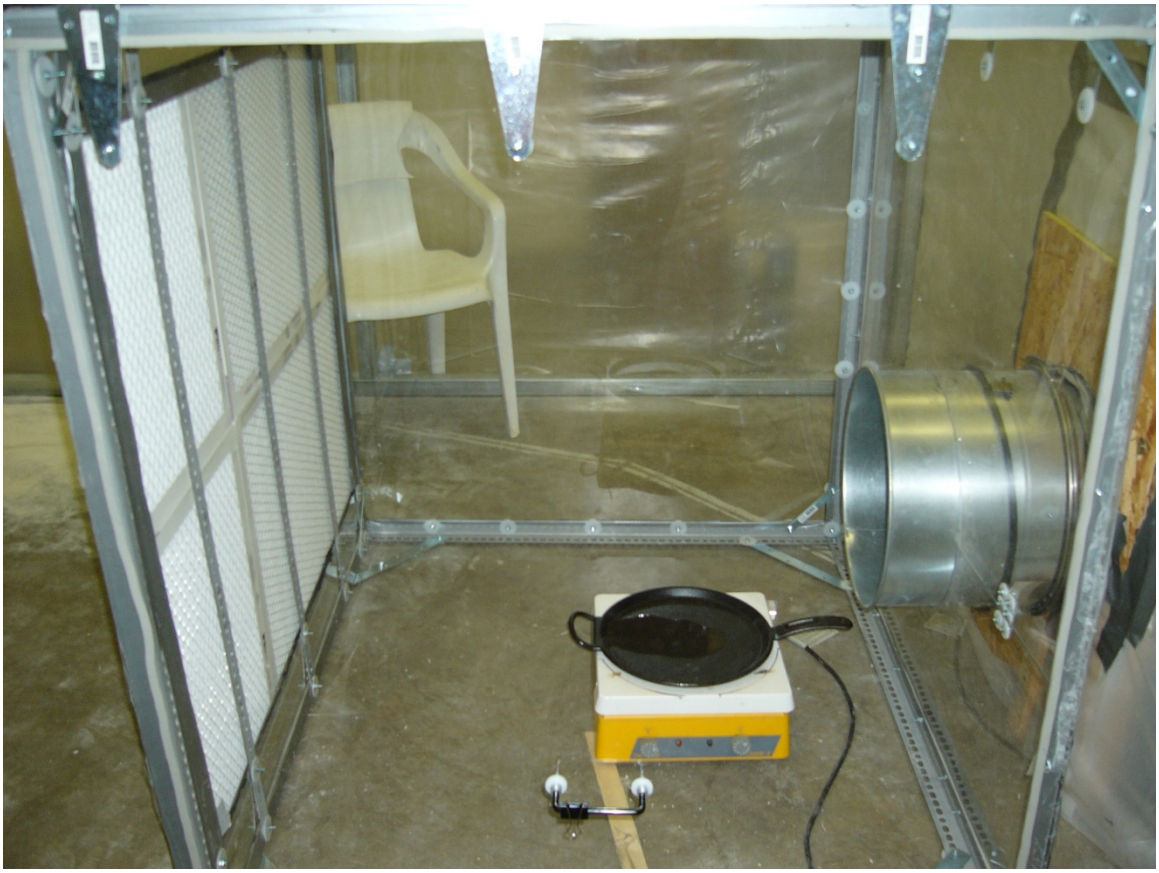

Figure 2-1 Side view of Enclosure

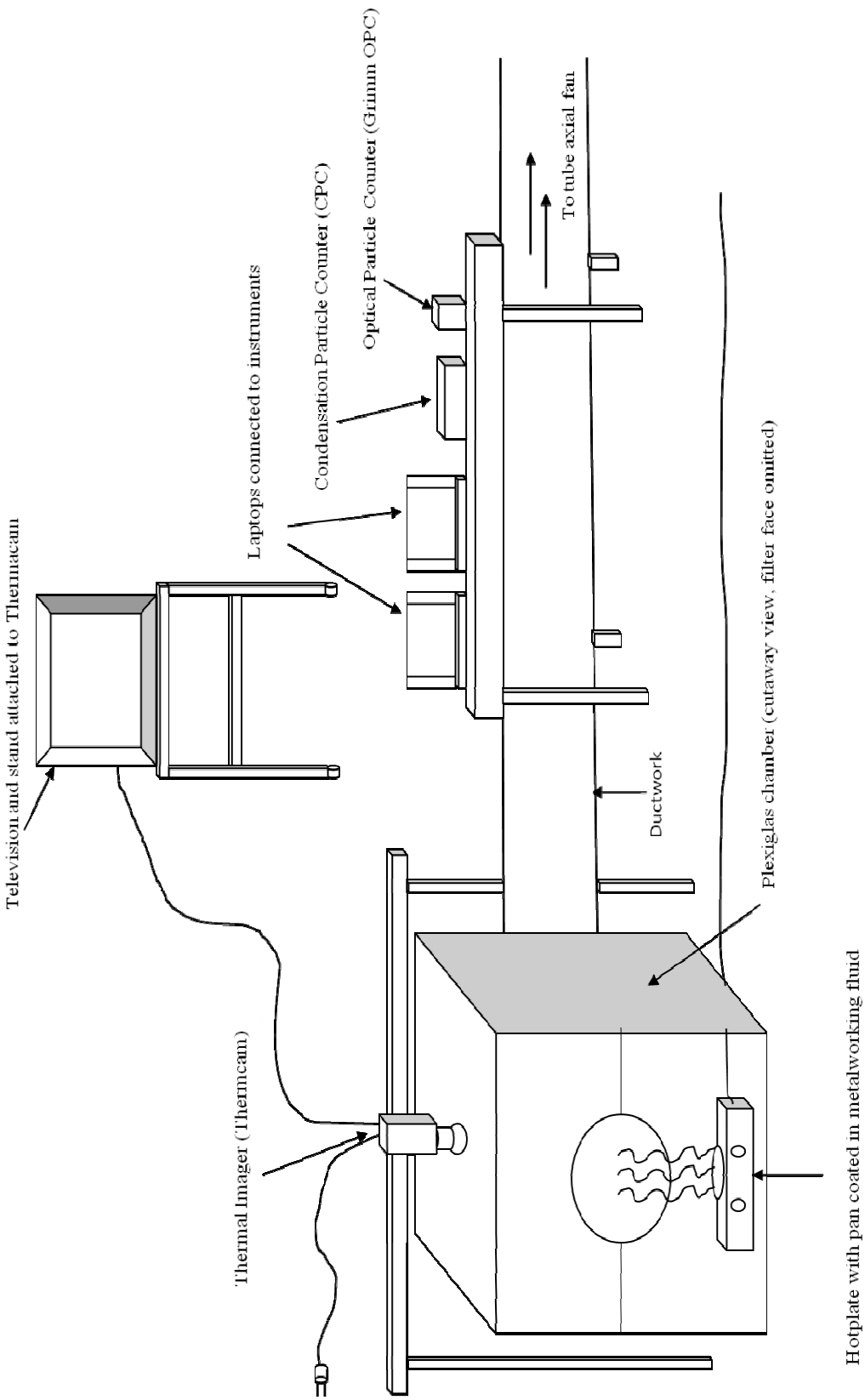

Figure 2-2 Schematic of Experimental Test Setup

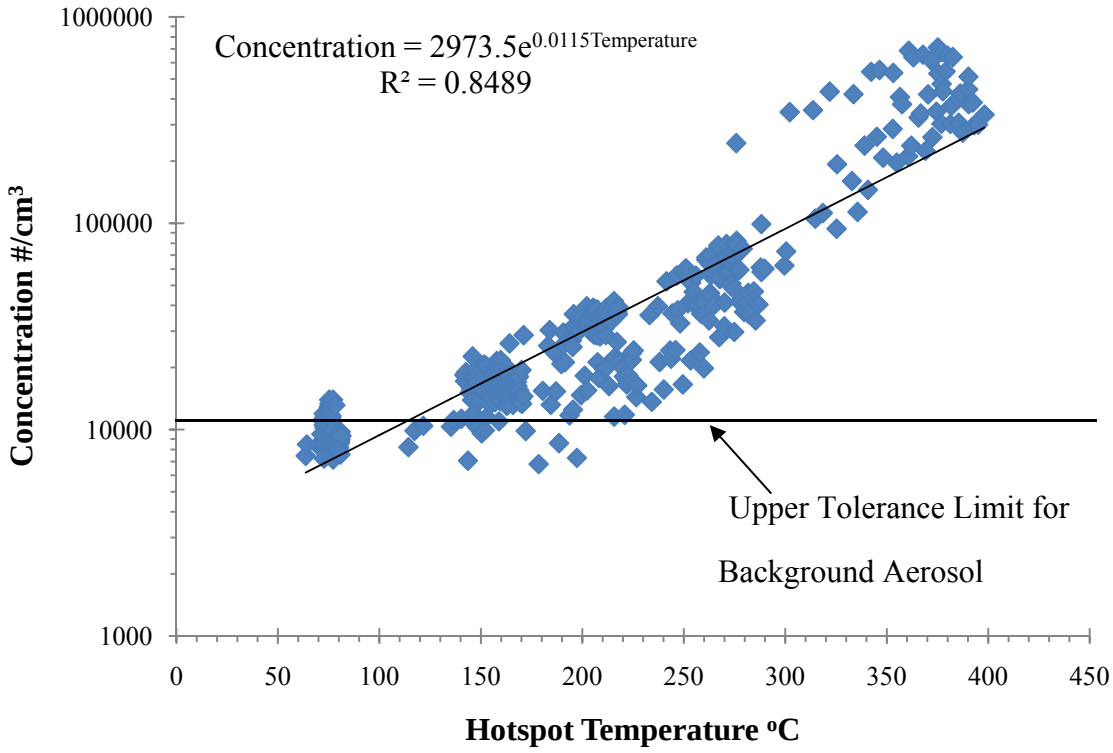

Figure 2-3 Concentration vs. Hotspot Temperature for Substance 1

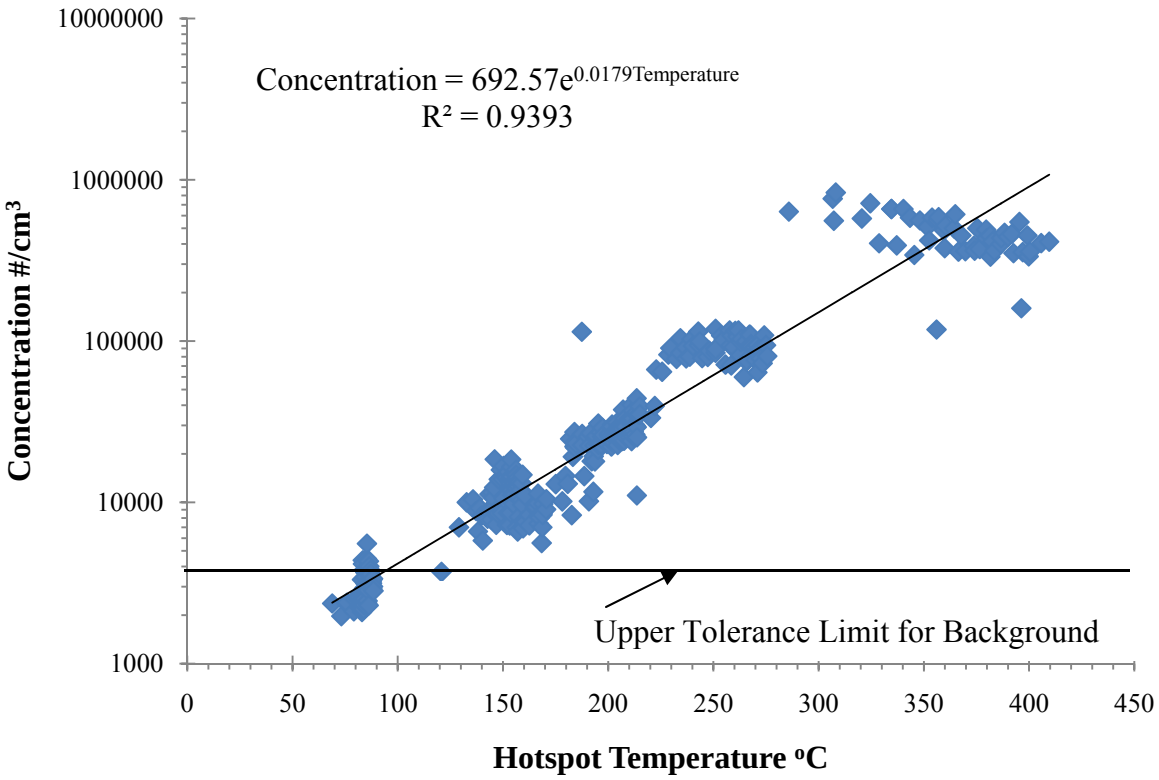

Figure 2-4 Concentration vs. Hotspot Temperature for Substance 2

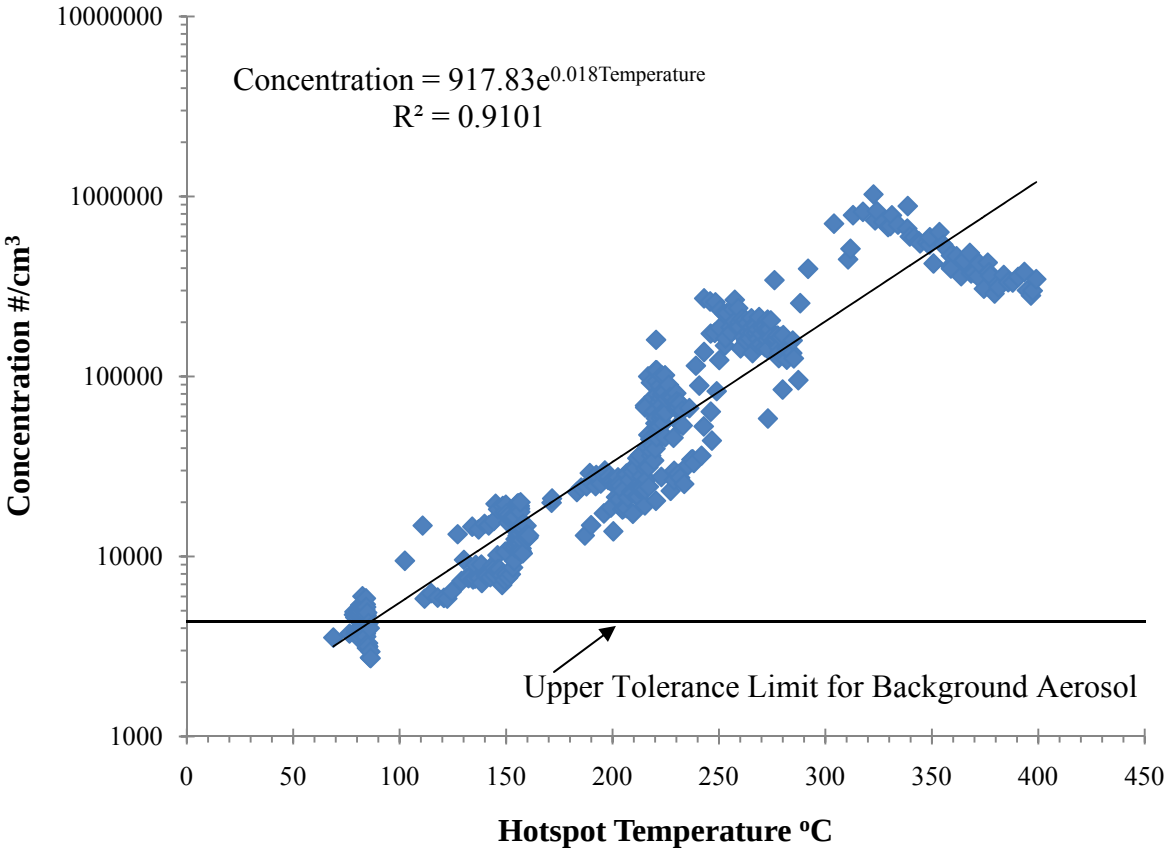

Figure 2-5 Concentration vs. Hotspot Temperature for Substance 3

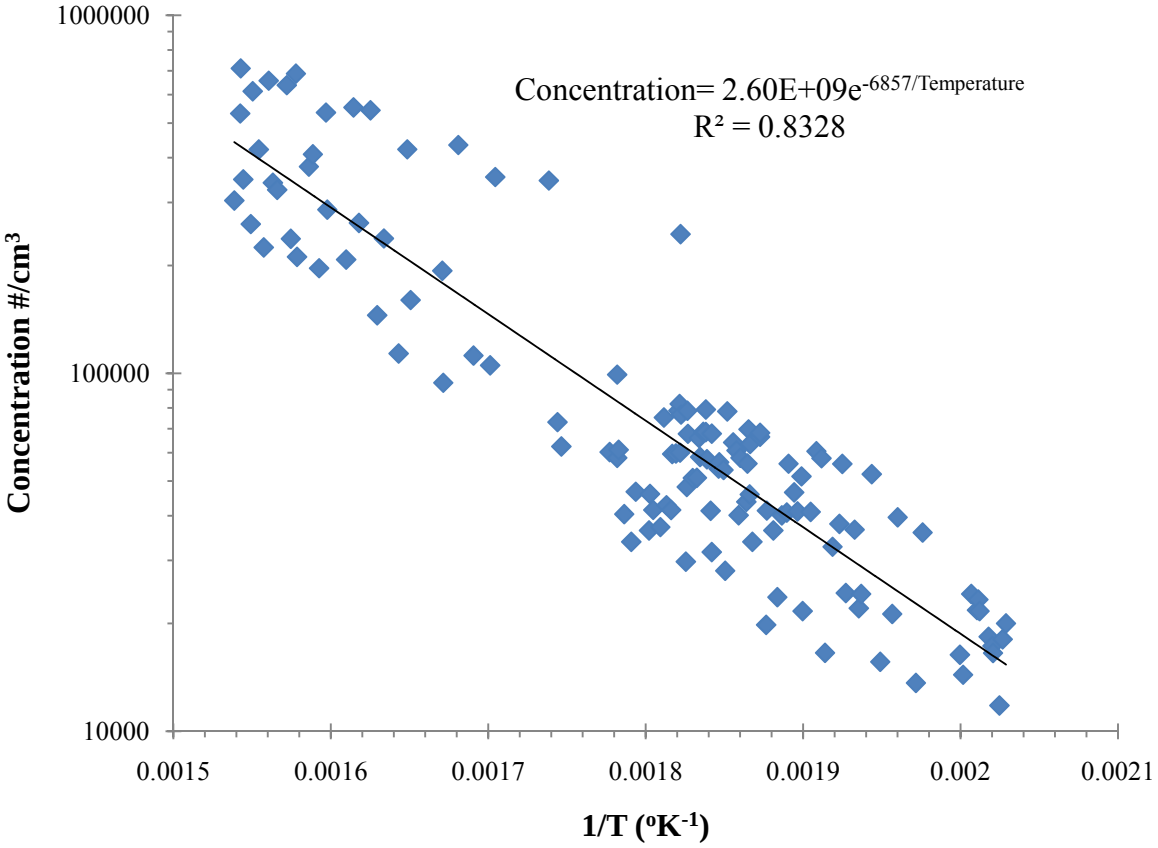

Figure 2-6 Concentration vs. Reciprocal Temperature Substance 1

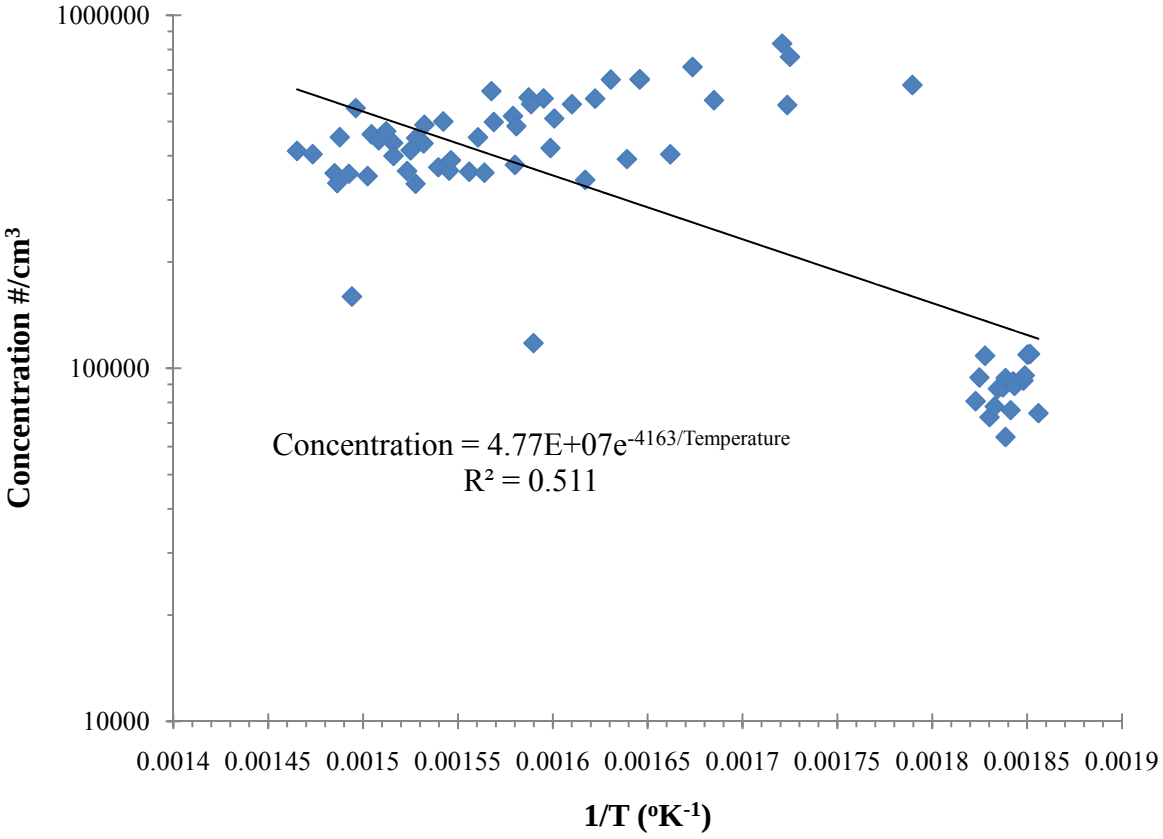

Figure 2-7 Concentration vs. Reciprocal Temperature Substance 2

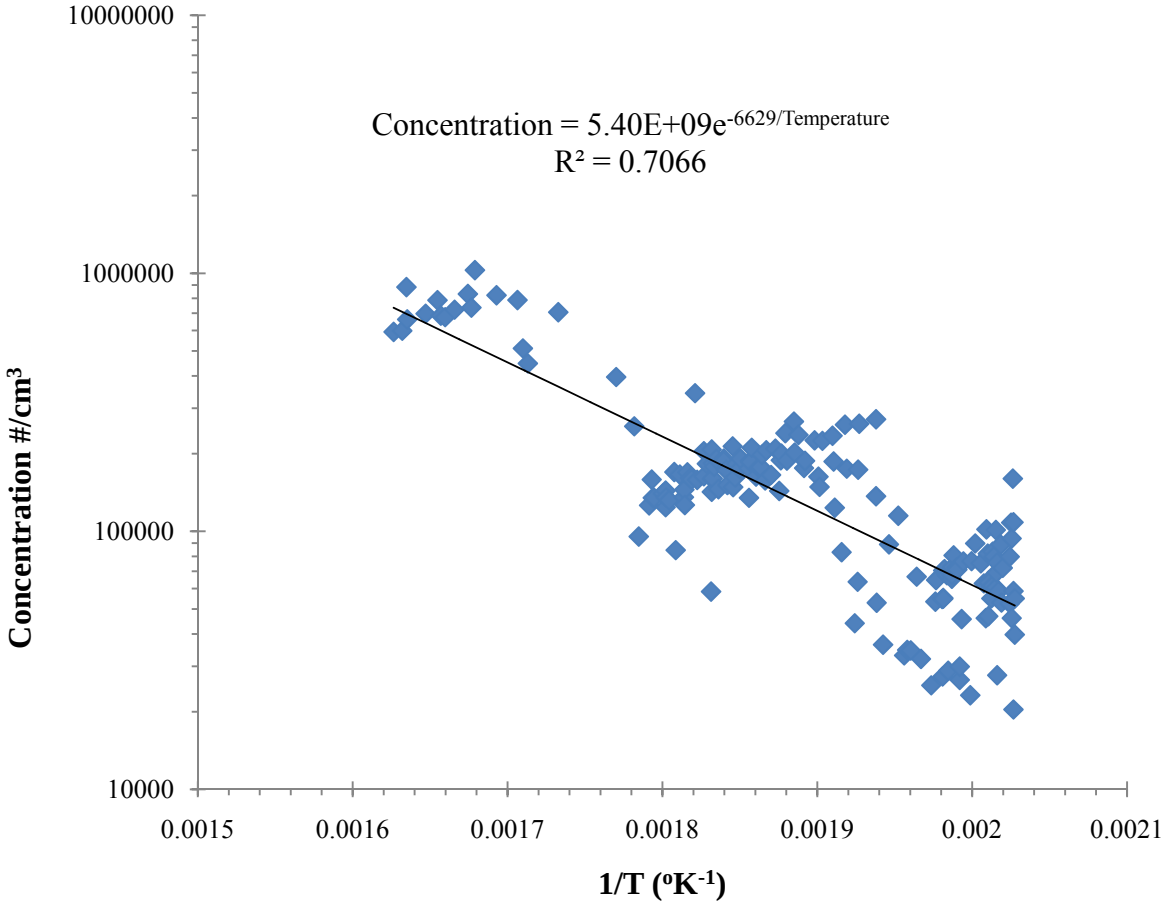

Figure 2-8 Concentration vs. Reciprocal Temperature Substance 3

CONCLUSIONS

Findings

Substances 1, 2, and 3 all follow the Clausius-Clapeyron equation to varying degrees and aerosol concentration is highly temperature dependant. Temperatures of greater than 150^{o}C are required to cause substantial burn-off to occur in an assembly plant, therefore surfaces that reach these temperatures should be washed to eliminate residues and prevent burn-off. The general particle size for this experiment is less than 2.0μm.

Future Research

Future research should be conducted to determine particle size distributions in all ranges. Temperatures greater than 300^{o}C should be analyzed using more than 5.00 grams of substance to determine if the higher temperatures also follow the Clausius-Clapeyron equation.

APPENDIX

Table A-1 Chemical and Physical Properties of Substances

	Substance 1	Substance 2	Substance 3
Listed Name	Laboratory Sample 52BRF-1	Laboratory Sample 52BRF-2	Laboratory Sample 52BRF-3
Generic Name	Synthetic Stamping and Drawing Lubricant	Water Soluble Metalworking Fluid Concentrate	Water Soluble Stamping and Drawing Fluid Concentrate
Hazardous Component	Triethanolamine CAS# 102-71-6	Triethanolamine CAS# 102-71-6	Hydro-treated Heavy Naphthenic Petroleum Distillates CAS# 64742-52-5
Percentage	1-5%	10-30%	15-40%
Hazardous Component	N/A	Aminomethylpropanol CAS# 124-68-5	Ethoxylated Fatty Amine CAS# 61791-26-2
Percentage	N/A	1-5%	1-5%
Hazardous Component	N/A	N/A	Synthetic Sodium Sulfonate CAS# 93820-59-8
Percentage	N/A	N/A	1-5%
Hazardous Component	N/A	N/A	Phosphated Alkyl Ethoxylated, Potassium Salt CAS# 154518-40-8
Percentage	N/A	N/A	1-5%
Hazardous Combustion Products	Smoke, fumes, oxides of nitrogen, and oxides of carbon	Smoke, fumes, oxides of nitrogen, oxides of phosphorus, oxides of sulfur, and oxides of carbon	Smoke, fumes, oxides of nitrogen, hydrogen chloride, and oxides of carbon
Flash Point	N/A	N/A	385°F (196.1°C)
Boiling Point	N/A	212°F (100°C)	N/A
Specific Gravity	0.98	1.05	1.06
Solubility (H_2O)	100%	100% Miscible	100% Miscible
pH (Concentrate)	N/A	8.7	N/A
pH (Mix)	7.7 @ 10%	8.5 @ 20%	8.5 @ 20%
Recommended Starting Dilution	Use Undiluted	5%	20%
Appearance/Odor	Opaque/Chemical	Clear/Chemical	Clear/Chemical
Evaporation Rate	N/A	Like water when diluted	Like water when diluted
Volatile Organic Content (by ASTM D2369)	N/A	6%	3%

Source: Cimcool, "Laboratory Sample 52BRF-1."Material Safety Data Sheet. 2007a, b, c.

Table A-2 Health Effects and Regulations of Substances

	Substance 1	Substance 2	Substance3
Listed Name	Laboratory Sample 52BRF-1	Laboratory Sample 52BRF-2	Laboratory Sample 52BRF-3
Generic Name	Synthetic Stamping and Drawing Lubricant	Water Soluble Metalworking Fluid Concentrate	Water Soluble Stamping and Drawing Fluid Concentrate
Acute Health Hazard	Yes	Yes	Yes
Chronic Health Hazard	No	No	No
Fire Hazard	No	No	Yes
Product Inhalation	N/A	Container vapor space may contain hydrogen sulfide. May cause respiratory irritation.	N/A
Product Eye Contact	Product is a primary eye irritant.	Product is a primary eye irritant.	Product is a primary eye irritant.
Product Skin Contact	Product may be a primary skin irritant.	Product may be a primary skin irritant.	Product may be a primary skin irritant.
Product Ingestion	Not orally toxic.	Not orally toxic.	Not orally toxic.
Product Dilution Inhalation	Extended exposure to mist may cause upper respiratory irritation.	Extended exposure to mist may cause upper respiratory irritation.	Extended exposure to mist may cause upper respiratory irritation.
Product Dilution Eye Contact	Will cause stinging sensation in the eye.	Will cause stinging sensation in the eye.	Will cause stinging sensation in the eye.
Product Dilution Skin Contact	Product may be a primary skin irritant.	Not irritation to the skin when used as directed and good personal hygiene is practiced.	Not irritation to the skin when used as directed and good personal hygiene is practiced.
Product Dilution Ingestion	Swallowing small quantities may cause diarrhea, nausea or vomiting.	Swallowing small quantities may cause diarrhea, nausea or vomiting.	Swallowing small quantities may cause diarrhea, nausea or vomiting.
Regulated Material	Triethanolamine	Triethanolamine	Metalworking fluid mist
Regulating Agency	ACGIH TLV	ACGIH TLV	NIOSH REL
Exposure Guideline	$0.5mg/m^3$	$0.5mg/m^3$	$0.5mg/m^3$
Regulated Material	Metalworking fluid mist	Metalworking fluid mist	Mineral oil (mist)
Regulating Agency	NIOSH REL	NIOSH REL	NIOSH REL, OSHA PEL, ACGIH TLV
Exposure Guideline	$0.5mg/m^3$	$0.5mg/m^3$	$5mg/m^3$

Source: Cimcool, "Laboratory Sample 52BRF-1."Material Safety Data Sheet. 2007a, b, c.

Table A-3 Substance 1 Hotspot Temperature Data

Run Number	Hotplate Setting	Number of Observations	Temperature Range	Concentration Range	Slope	Slope Standard Error	R^2 Value	Adjusted R^2	R^2 Standard Error	Intercept Coefficient	Intercept Standard Error
1	2	47	64-78	1034-1994	-5417.1	1046.28	0.37	0.36	0.14	22.91	3.01
2	2	37	72.5-80.2	1023-1557	4688.9	997.75	0.39	0.37	0.08	-6.26	2.85
3	2	22	64.2-81.3	1082-1395	-482.52	553.6	0.04	-0.01	0.07	8.5	1.57
4	4	38	99.3-162.9	1088-3234	-2181.2	309.23	0.58	0.57	0.15	12.95	0.73
5	4	22	114.3-164.5	1176-2826	-2470.4	397.62	0.66	0.64	0.13	13.4	0.93
6	4	41	143.6-171.1	1010-4099	-3765.2	895.09	0.31	0.29	0.21	16.31	2.05
7	6	29	180.5-211.7	2205-5656	-3300	584.84	0.54	0.52	0.13	15.37	1.23
8	6	29	172.1-217.3	1407-6002	-5981.6	610.21	0.78	0.77	0.17	20.9	1.28
9	6	29	178.5-227.1	973-4240	-3771.6	862.56	0.41	0.39	0.25	15.59	1.78
10	8	29	150.5-281.1	3608-10746	-1511.5	269.41	0.54	0.52	0.18	11.75	0.51
11	8	24	215.7-276.2	1653-11737	-9039.2	560.68	0.92	0.92	0.14	25.87	1.05
12	8	29	197.3-289.7	1043-14167	-6436.6	604.08	0.81	0.8	0.24	20.39	1.12
13	10	19	275.8-382.5	34948-101566	-3207.2	357.86	0.83	0.82	0.12	16.36	0.58
14	10	21	258.6-398.2	5196-54950	-6266.2	345.37	0.95	0.94	0.15	20.2	0.55
15	10	20	262.9-390.2	6553-73272	-6922.3	417.22	0.94	0.94	0.17	21.6	0.67

Table A-4 Substance 1 Average Temperature Data

Run Number	Hotplate Setting	Number of Observations	Temperature Range	Concentration Range	Slope	Slope Standard Error	R^2 Value	Adjusted R^2	R^2 Standard Error	Intercept Coefficient	Intercept Standard Error
1	2	47	46.4-73.5	1034-1994	-2687.60	638.59	0.28	0.27	0.15	15.17	1.87
2	2	37	65.4-74.7	1023-1557	3781.10	742.45	0.43	0.41	0.08	-3.86	2.16
3	2	22	47.7-74.8	1082-1395	-227.99	328.01	0.02	-0.03	0.08	7.79	0.95
4	4	38	67.0-142.3	1088-3234	-1826.90	213.36	0.67	0.66	0.13	12.31	0.53
5	4	22	71.4-140.7	1176-2826	-1507.70	254.00	0.64	0.62	0.13	11.37	0.64
6	4	41	106.7-149.6	1010-4099	-2736.20	502.37	0.43	0.42	0.19	14.28	1.21
7	6	29	126.1-180.7	2205-5656	-2371.10	269.85	0.74	0.73	0.10	13.76	0.61
8	6	29	116.2-187.3	1407-6002	-3532.40	238.34	0.89	0.89	0.12	16.31	0.54
9	6	29	121.4-193.3	973-4240	-2678.50	446.22	0.57	0.56	0.21	13.76	0.99
10	8	29	100.7-233.0	3608-10746	-1082.50	200.48	0.52	0.50	0.18	11.13	0.42
11	8	24	142.5-228.2	1653-11737	-4830.10	291.67	0.93	0.99	0.14	18.92	0.61
12	8	29	134.0-240.0	1043-14167	-4355.80	488.39	0.75	0.74	0.28	17.30	0.99
13	10	19	137.4-333.1	34948-101566	-1351.00	189.47	0.75	0.73	0.15	13.60	0.34
14	10	21	137.4-336.0	5196-54590	-3199.30	343.82	0.82	0.81	0.27	15.89	0.61
15	10	20	108.5-301.8	6533-73272	-2677.70	168.24	0.93	0.93	0.17	15.65	0.32

Table A-5 Substance 2 Hotspot Temperature Data

Run Number	Hotplate Setting	Number of Observations	Temperature Range	Concentration Range	Slope	Slope Standard Error	R^2 Value	Adjusted R^2	R^2 Standard Error	Intercept Coefficient	Intercept Standard Error
1	2	20	68.9-86.2	328-378	-108.74	300.03	0.01	-0.05	0.04	6.16	0.84
2	2	27	73.2-85.7	281-625	-4938.80	1634.30	0.27	0.24	0.20	19.84	4.59
3	2	27	81.6-88.5	353-792	-102.46	251.38	0.01	-0.03	0.19	6.48	0.71
4	4	41	129.1-170.5	798-1615	342.77	296.69	0.02	-0.01	0.16	6.29	0.93
5	4	29	140.4-159.3	367-2113	-6642.70	868.90	0.68	0.67	0.12	22.93	2.03
6	4	27	120.8-157.2	528-2640	-6582.80	754.21	0.75	0.74	0.17	23.10	1.79
7	6	37	165.0-207.5	1317-5358	-4631.90	581.33	0.64	0.63	0.18	18.04	1.25
8	6	32	182.7-215.0	1188-6295	-7655.80	1021.64	0.65	0.64	0.19	24.22	2.13
9	6	29	178.2-213.6	1447-5740	-6601.10	647.08	0.79	0.79	0.13	22.05	1.36
10	8	28	187.5-275.6	1576-17036	-2167.10	988.50	0.16	0.12	0.43	13.51	1.89
11	8	13	188.8-256.0	3424-16842	-1807.90	1234.44	0.16	0.09	0.41	13.00	2.39
12	8	23	192.9-272.1	1658-14660	-4183.00	956.99	0.48	0.45	0.33	17.26	1.83
13	10	17	307.2-399.8	22810-82092	2188.60	790.61	0.34	0.29	0.23	7.46	1.24
14	10	17	306.7-409.5	51022-108996	2537.80	312.05	0.82	0.80	0.10	7.23	0.49
15	10	17	285.8-390.0	47595-118846	2496.10	543.65	0.58	0.56	0.16	7.23	0.86

Table A-6 Substance 2 Average Temperature Data

Run Number	Hotplate Setting	Number of Observations	Temperature Range	Concentration Range	Slope	Slope Standard Error	R^2 Value	Adjusted R^2	R^2 Standard Error	Intercept Coefficient	Intercept Standard Error
1	2	20	54.6-82.5	328-378	-100.53	176.65	0.02	-0.04	0.04	6.14	0.50
2	2	27	61.0-80.8	281-625	-2990.30	1075.70	0.24	0.21	0.20	14.49	3.06
3	2	27	75.9-84.2	353-792	-2740.60	2226.52	0.06	0.02	0.19	13.92	6.27
4	4	41	116.7-152.1	798-1615	368.31	449.86	0.02	-0.01	0.16	6.20	1.09
5	4	29	107.3-141.8	367-2113	-3507.50	415.60	0.73	0.71	0.11	15.96	1.02
6	4	27	91.0-141.6	528-2640	-4168.20	365.65	0.84	0.83	0.14	17.79	0.90
7	6	37	126.2-185.1	1317-5358	-3499.30	342.28	0.75	0.74	0.15	15.99	0.77
8	6	32	128.8-187.4	1188-6295	-4208.40	421.99	0.77	0.76	0.16	17.61	0.94
9	6	29	132.6-186.3	1447-5740	-3722.70	350.60	0.81	0.80	0.12	16.51	0.78
10	8	28	164.8-228.8	1576-17036	-4647.90	818.59	0.55	0.54	0.32	18.96	1.69
11	8	13	107.3-220.9	3424-16842	-918.25	656.95	0.15	0.07	0.41	11.48	1.42
12	8	23	136.8-226.9	1658-14660	-3360.20	573.21	0.62	0.60	0.28	16.27	1.20
13	10	17	215.9-303.6	22810-82092	1694.90	663.12	0.30	0.26	0.24	7.81	1.21
14	10	17	212.9-317.0	51022-108996	1951.10	288.22	0.75	0.74	0.11	7.71	0.51
15	10	17	210.7-303.4	47595-118846	1894.10	373.63	0.63	0.61	0.15	7.72	0.69

Table A-7 Substance 3 Hotspot Temperature Data

Run Number	Hotplate Setting	Number of Observations	Temperature Range	Concentration Range	Slope	Slope Standard Error	R^2 Value	Adjusted R^2	R^2 Standard Error	Intercept Coefficient	Intercept Standard Error
1	2	22	82.6-86.4	389-858	19855.00	4928.45	0.45	0.42	0.18	-49.21	13.78
2	2	32	68.9-84.2	501-585	-897.17	271.73	0.27	0.24	0.03	8.84	0.77
3	2	22	78.6-84.8	649-776	-1614.10	747.08	0.19	0.15	0.05	11.11	2.11
4	4	40	111.7-157.9	833-1866	-2325.70	234.21	0.72	0.71	0.11	12.67	0.56
5	4	22	102.5-159.6	1271-2161	-1581.40	326.29	0.53	0.50	0.12	11.05	0.77
6	4	30	110.8-160.8	1781-2861	-378.54	412.10	0.03	0.02	0.14	8.98	0.98
7	6	42	171.6-224.8	2995-12670	-5517.80	829.16	0.57	0.58	0.27	21.56	1.71
8	6	41	171.4-232.9	2841-22849	-5778.60	895.34	0.52	0.51	0.38	20.96	1.82
9	6	28	157.0-225.1	1688-10944	-6660.00	1180.90	0.55	0.52	0.38	21.71	2.45
10	8	25	187.0-276.8	1867-29645	-8257.60	584.92	0.90	0.89	0.27	25.54	1.13
10 Redo	8	32	200.4-276.1	1969-49034	-11789.00	1299.51	0.73	0.72	0.53	32.23	2.49
11	8	23	155.7-284.5	2000-26927	-5308.50	800.68	0.68	0.66	0.42	19.63	1.51
12	8	26	229.0-285.2	4269-28863	-7167.40	1310.55	0.55	0.54	0.36	23.08	2.43
13	10	12	317.7-385.9	44662-117415	5106.00	415.61	0.94	0.93	0.08	3.07	0.66
14	10	21	288.2-399.1	36476-118693	1674.70	810.59	0.18	0.14	0.29	8.32	1.28
14 Redo	10	12	279.9-364.5	12077-112461	-3650.90	2147.35	0.22	0.15	0.55	17.24	3.58
15	10	14	273.0-379.5	8341-146925	-4378.40	2109.45	0.26	0.20	0.70	18.04	3.45

Table A-8 Substance 3 Average Temperature Data

Run Number	Hotplate Setting	Number of Observations	Temperature Range	Concentration Range	Slope	Slope Standard Error	R^2 Value	Adjusted R^2	R^2 Standard Error	Intercept Coefficient	Intercept Standard Error
1	2	22	76.4-81.8	389-858	16899.00	2781.62	0.65	0.63	0.15	-41.60	7.89
2	2	32	57.5-79.7	501-585	-572.47	183.94	0.24	0.22	0.04	7.94	0.53
3	2	22	74.3-80.7	649-776	-1453.40	664.59	0.19	0.15	0.05	10.71	1.90
4	4	40	85.8-138.9	833-1866	-2092.20	255.82	0.64	0.63	0.13	12.32	0.64
5	4	22	67.7-147.9	1271-2161	-1020.00	188.81	0.59	0.56	0.11	9.88	0.47
6	4	30	75.5-139.1	1781-2861	-368.34	276.09	0.05	0.05	0.14	8.77	0.69
7	6	42	117.2-184.7	2995-12670	-3372.60	974.54	0.34	0.38	0.32	19.69	2.17
8	6	41	113.1-192.5	2841-22849	-4151.80	755.91	0.44	0.43	0.41	18.28	1.67
9	6	28	102.2-185.3	1688-10944	-3447.40	867.43	0.37	0.34	0.45	15.80	1.95
10	8	25	125.8-223.6	1867-29645	-6758.30	540.56	0.87	0.87	0.30	23.88	1.15
10 Redo	8	32	137.3-220.8	1969-49034	-9489.50	1152.38	0.69	0.68	0.57	29.62	2.42
11	8	23	115.6-229.6	2000-26927	-4963.40	583.22	0.78	0.76	0.35	19.95	1.12
12	8	26	160.4-229.1	4269-28863	-6276.30	764.89	0.74	0.73	0.28	22.66	1.57
13	10	12	203.5-298.4	44662-117415	2726.50	378.60	0.84	0.82	0.13	6.13	0.70
14	10	21	121.7-316.1	36476-118693	304.00	325.25	0.04	-0.01	0.32	10.39	0.61
14 Redo	10	12	136.6-279.8	12077-112461	-1795.50	722.28	0.38	0.32	0.49	14.75	1.45
15	10	14	130.7-295.9	8341-146925	-2128.20	906.21	0.31	0.26	0.68	15.01	1.76

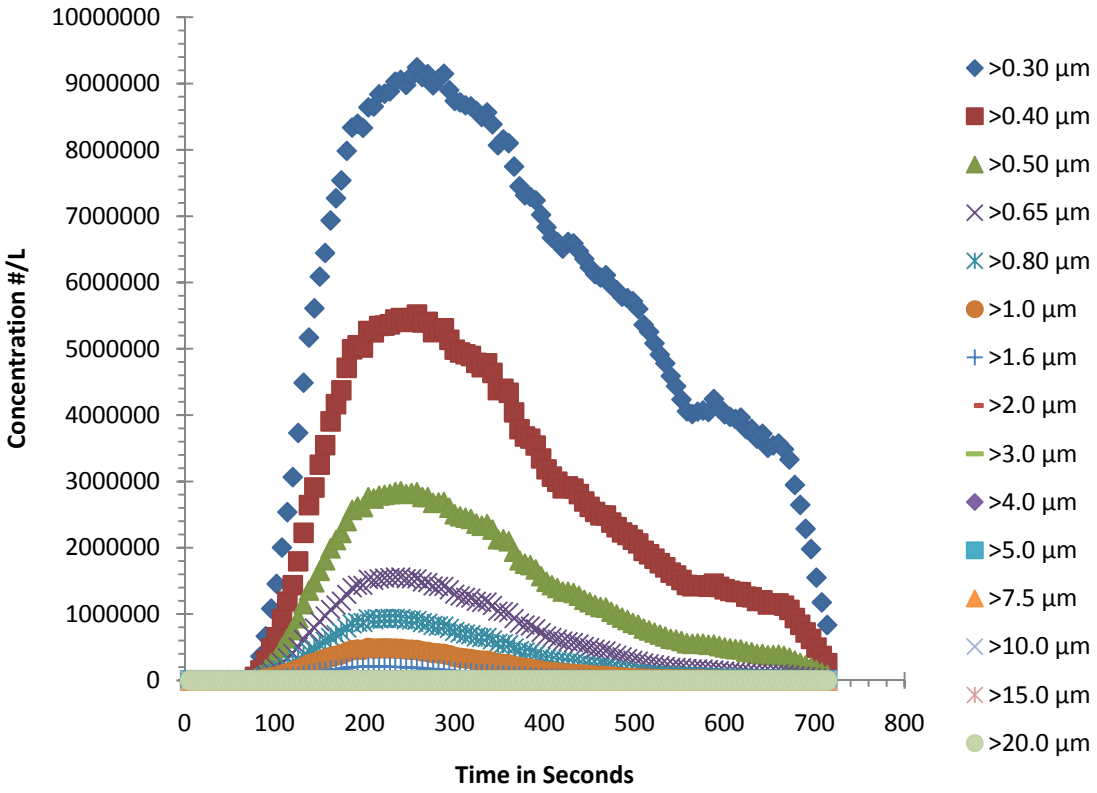

Figure A-1 Optical Particle Counter Output Substance 1 Run 15

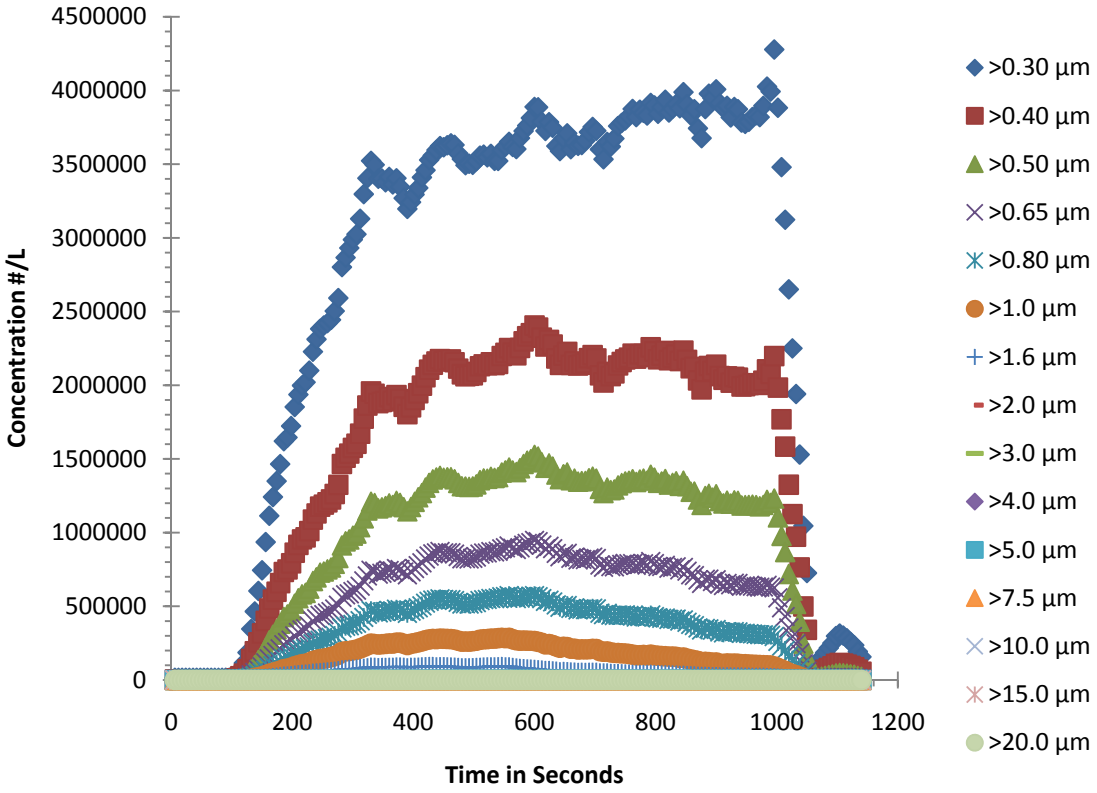

Figure A-2 Optical Particle Counter Output Substance 2 Run 9

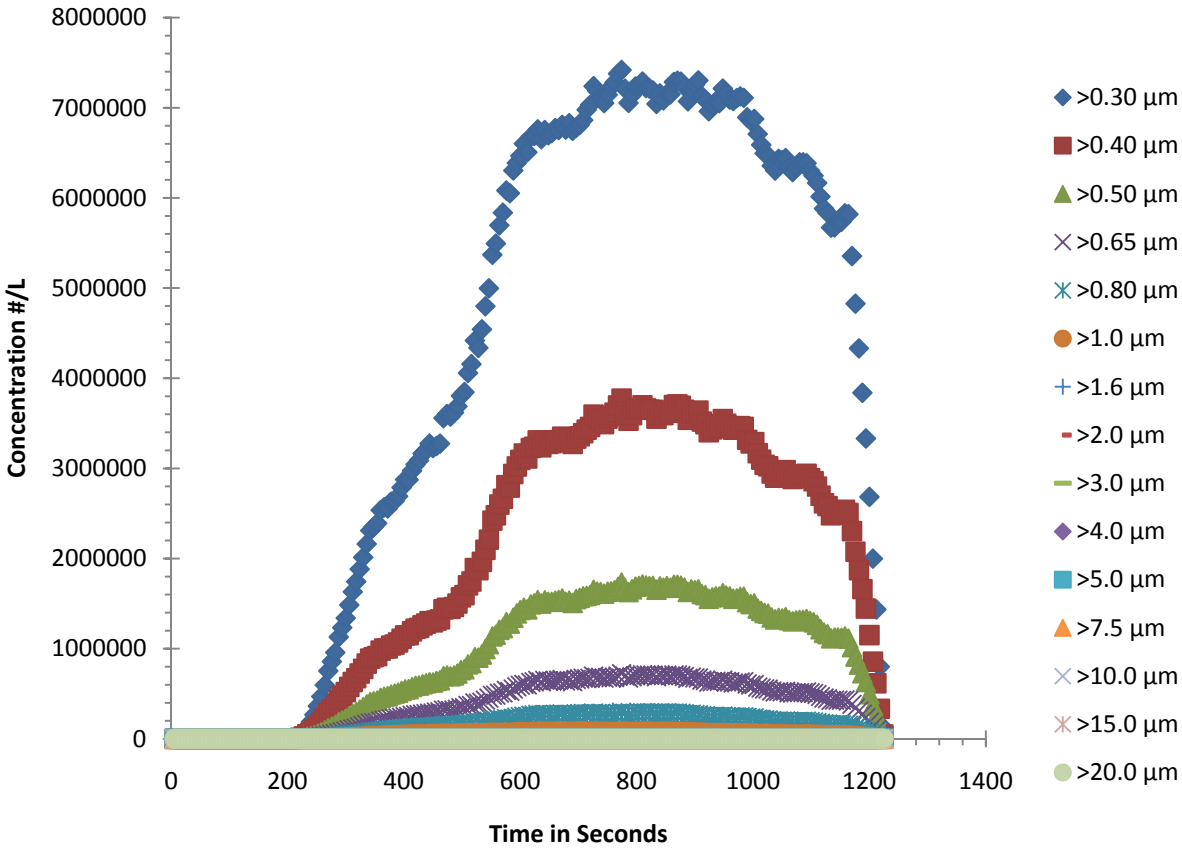

Figure A-3 Optical Particle Counter Output Substance 3 Run 10

REFERENCES

Anderson, H. R.. "Differential epidemiology of ambient aerosols." Phil. Trans. R. Soc. Lond. 358(2000): 2771-2785.

Bird, R., Stewart, W., & Lightfoot, E. (1966). Transport phenomena. New York: John Wiley & Sons, Inc..

Brouwer, Derk H., Gijsbers, Jose H. J., Lurvink, Marc W. M.. "Personal Exposure to Ultrafine Particles in the Workplace: Exploring Sampling Techniques and Strategies." Ann. Occup. Hyg. 48(2004): 439-453.

Castellan, Gilbert W. (1966). Physical chemistry. Reading, MA: Addison-Wesley Publishing Company.

Cimcool, "Laboratory Sample 52BRF-1."Material Safety Data Sheet. 2007a.

Cimcool, "Laboratory Sample 52BRF-2."Material Safety Data Sheet. 2007b.

Cimcool, "Laboratory Sample 52BRF-3."Material Safety Data Sheet. 2007c.

Detwiler-Okabayashi, Katherine A., Schaper, Michelle M.. "Respiratory effects of a synthetic metalworking fluid and its components." Arch Toxicol 70(1996): 195-201.

Donaldson, K., Stone, V., Gilmour, S., Brown, D. M., MacNee, W.. "Ultrafine Particles: Mechanisms of Lung Injury." Philosophical Transactions: Mathematical, Physical and Engineering Sciences 358(2000): 2741-2749.

Dougherty, Edward R. (1990). Probability and statistics for the engineering, computing and physical sciences. Englewood Cliffs, NJ: Prentice Hall.

Fairchild, Ray, M., Snyder, Rick B., Berlin, Carl W., Sarma, D. H. R.. "Emerging Substrate Technologies for Harsh-Environment Automotive Electronics Applications." Society of Automotive Engineers Technical Paper Series 2002-01-1052(2002):

FLIR Systems. (1999). ThermaCAM Model PM390 Operation Manual [Brochure]. North Billerica, MA.

FLIR Systems, Inc., "IR Thermography Primer." Infrared Training Center. 2005. 14 Jun 2007 <http://www.infraredtraining.com/ir_primer.asp>.

Grimm technologies, Inc.. (2002). GRIMM Dust Monitor Series 1.100 Operator's Manual [Brochure]. Douglasville, GA:

Highwood, Eleanor J., Kinnersley, Robert P.. "When smoke gets in our eyes: the multiple impacts of atmospheric black carbon on climate, air quality and health." Science Direct Environmental International (2006): 1-8.

Hinds, William C. (1999). Aerosol technology: Properties, behavior, and measurement of airborne particles. New York, NY: John Wiley & Sons, INC..

Johnson, R. Wayne, Evans, John L. Jacobsen, Peter, Thompson, James R. (Rick), Christopher, Mark. "The Changing Automotive Environment: High-Temperature Electronics." IEEE Transactions on Electronics Packaging Manufacturing 27(2004): 164-176.

Kreyling, Wolfgang G., Semmler-Behnke, Manuela, Moller, Winfried. "Health implications of nanoparticles." Journal of Nanoparticle Research 8(2006): 543-562.

Lide, David R. (1992). CRC Handbook of Chemistry & Physics 73rd Edition. Boca Raton, FL: CRC Press.

McCawley, Michael A., Kent, Michael S., Berakis, Michael T.. "Ultrafine Beryllium Number Concentration as a Possible Metric for Chronic Beryllium Disease Risk." Applied Occupational and Environmental Hygiene 16(2001): 631-638.

Natrella, Mary G. (1963). Experimental Statistics National Bureau of Standards Handbook 91 . Washington, D.C.: United States Department of Commerce.

Nicholas, J. V., White, D. R. . Traceable Temperatures . 2. Chichester: Wiley, 2001.

NIOSH, "Metalworking fluids NIOSH Topic Page." CDC. 2006 . 21 Aug 2007 <http://www.cdc.gov/niosh/topics/metalworking/>.

NIOSH, "Safety and Health Topics: Metalworking fluids- Health Effects." U. S. Department of Labor Occupational Safety and Health Administration. 2005. OSHA. 21 Aug 2007 <http://www.osha.gov/STLC/metalworkingfluids/health_effects.html>.

Oberdörster, Gunter. "Pulmonary effects of inhaled ultrafine particles." Int Arch Occup Environ Health 74(2001): 1-8.

O'Brien , Dennis M.. "Aerosol Mapping of a Facility with Multiple Cases of Hypersensitivity Pneumonitis: Demonstration of Mist Reduction and a Possible Dose/Response Relationship." Applied Occupational and environmental Hygiene 18(2003): 947-952.

Ostiguy, C., Lapointe, G., Trottier, M., Ménard, L., Cloutier, Y., Boutin, M., Antoun, M., & Normand, C. (2006). Health Effects of Nanoparticles. IRSST 6-13.

Park, Robert M. Krebs, Jane M., Krebs, Franklin E.. "Occupational Disease Surveillance Using Disability Insurance at an Automotive Stamping and Assembly Complex." Journal of Occupational and Environmental Medicine 38(1996): 1111-1123.

Peters TM, Heitbrink WA, Evans DE et al. (2006) The mapping of fine and ultrafine particles in an engine machining and assembly facility. Ann Occup Hyg; 50: 249–57.

Poling, B., Prausnitz, J., & O'Connell, J. (2000). The properties of gases and liquids. New York: McGRAW-HILL.

Society of Tribologists and Lubrication Engineers, Metalworking Fluids . 2. Wakefield: CRC Press Taylor & Francis, 2006.

TSI Incorporated. (2004). Model 3007 Condensation Particle Counter Operation and Service Manual (D ed.) [Brochure]. Shoreview, MN

Vincent, James H., Clement, Charles F.. "Ultrafine particles in workplace atmospheres." Phil. Trans. R. Soc. Lond. 358(2000): 2673-2682.

Wichmann, H.-Erich, Peters, Annette. "Epidemiological Evidence of the Effects of Ultrafine Particles Exposure." Philosophical Transactions: Mathematical, Physical and Engineering Sciences 358(2000): 2751-2769.